

Explosion induced structural response: An overview

R. P. Dhakal

Department of Civil Engineering, University of Canterbury, Christchurch.



2004 NZSEE
Conference

ABSTRACT: This paper presents a conceptual discussion on structural response to ground shocks. Nonlinear finite element analyses on a 2storey RC frame subjected to explosion-induced ground shocks are carried out to investigate structural response to explosions. This study shows that maximum response to explosion generally occurs after the major ground shock has ceased. It is found that the response in the forced-vibration phase includes high frequency vibration modes characterised by small displacement but large acceleration, which induce high inertial shear force. On the other hand, the free-vibration response is dominated by lower frequency oscillations with large displacement which may soften the structure. Hence, a structure subjected to explosion may have to face two probable hazards. Firstly, it may experience a large shear force that may cause a sudden shear failure within the major shock period. Secondly, if its shear resistance is large enough to overcome the induced shear force, it may undergo large flexural deformation that may induce severe damage after the major ground shock has ceased. The possibility and extent of these two damage mechanisms depend on the scale of explosion, the distance of the structure from the explosion source and the toughness of the structure.

1 INTRODUCTION

Response of residential structures to natural disasters such as earthquakes and strong winds has been studied extensively, and the outcomes of such studies have been well documented. Based on the results of these studies, design codes for high-seismicity regions and wind-prone countries have been amended to safeguard structures from earthquakes and winds. On the other hand, comparatively fewer studies have been found on structural response to explosions despite that their probability of occurrence is higher compared to that of earthquakes and windstorms. The increasing frequency of car bomb or human bomb attacks at public places throughout the world in recent years and, of course, the September 11 terrorist attack on the twin towers of New York's World Trade Centre have further underscored the need to incorporate anti-explosion safety criteria in structural design. Lack of sufficient research in this field has frustrated many terrorism stricken countries as they are unable to amend their design regulations to fully safeguard the structures from terrorist attacks. Encouragingly, many researchers seemed to be attracted to this field recently, and some investigations are being carried out, which will certainly help to add a new dimension in the form of blast resistance to building design.

The major sources of ground shocks are construction related explosions, accidental detonation of stored explosives, terrorist attacks, and bombs used during wars. A ground shock generated by an underground or a surface explosion propagates from the source to the base of a structure through the surrounding soil media. Although the propagation and attenuation of such ground shocks are qualitatively similar to those of seismic waves, the specific features of a ground shock induced by explosions are different from those of an earthquake-induced excitation. Consequently, structural response to such ground shocks will also be somewhat different from structural response to earthquakes, and fresh study is needed to assess the nature of potential damage to be incurred on a structure when subjected to explosions. This paper highlights the special features of explosion induced ground shocks and explores the basic response characteristics of structures subjected to such ground shocks. By means of numerical analyses, basic damage mechanisms of structures subjected to

explosions are identified, and a conceptual hazard attenuation curve for a typical structure is generated.

2 EXPLOSION-INDUCED GROUND SHOCKS

The magnitude of a ground shock induced by explosion depends on many factors such as quality and quantity of explosives, depth of charge, properties of the surrounding soil, distance from the explosion source, etc. Although ground shocks recorded from medium to large scale explosions are scarce, there have been a few attempts to generate such ground shocks synthetically [Ma et al 1998]. The limited available records indicate that explosion-induced ground shocks possess three unique characteristics: short duration, large amplitude and high frequency. As a representative case, the acceleration time history of an explosion-induced ground shock and its Fourier transform are shown in Figure 1. Note that the peak ground acceleration (PGA) of this shock is 1220.19 m/s^2 and the effective shock duration containing substantial acceleration amplitude is less than 0.05 sec. Moreover, it includes significant higher frequency components, and the peak Fourier amplitude corresponds to 188.65 Hz. Compare these with the corresponding values for seismic excitations (duration >10 sec; PGA < 1g; frequency < 5 Hz), and it becomes evident that these two cannot be bracketed in the same category.

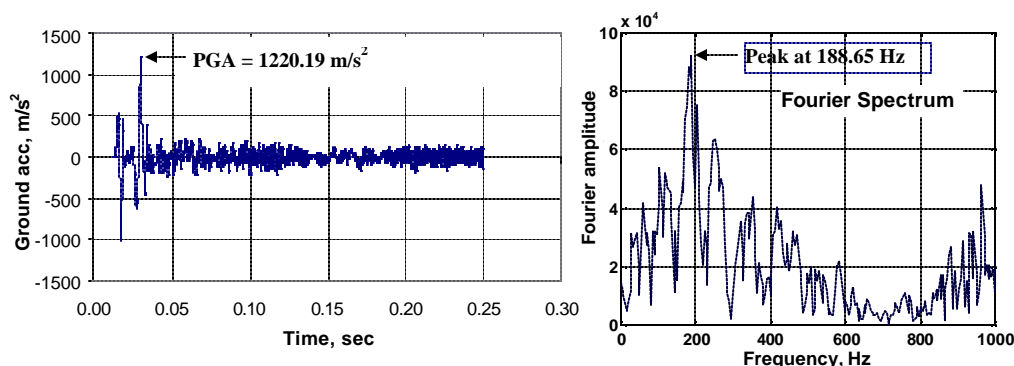


Figure 1 Typical explosion-induced ground shock

The attenuation of ground shock characteristics with respect to distance have also been investigated [Pan et al 2003]. It was concluded that PGA and PPV (peak particle velocity) of such ground shocks decrease with an increase in distance but the reduction rate becomes less prominent as the distance increases. It was also found that the very high frequency components gradually disappear as the distance increases, but the dominant frequency band remains more-or-less the same. It is also obvious that the amplitude will decrease as the amount of explosive reduces. Assuming ambient conditions remain same, a ground shock may hence represent various combinations of explosive quantity and distance from detonation. This agrees with the quantity-distance theory which is used to calculate IBD (inhabited building distance) in existing ammunition storage guidelines [NATO 1970, DoD 1992]. In quantity-distance theory, the ground shock hazard distance is proportional to an exponential of the explosive quantity. This originates from an assumption that the PPV of an explosion-induced ground shock is proportional to Q^k/D^l where Q is the explosive quantity, D is the distance from the explosion source, and k and l are constants.

The short-duration (less than 0.1 s) renders the explosion-induced ground shocks of impulsive nature, and the maximum response of normal structures with natural frequency less than 5 Hz hence occurs after the major shocks have ceased; i.e. in the free-vibration phase. Hence, the time covered in the numerical computation of structural response to a ground shock should be a few times longer than the major shock duration. The analysis within only the major shock duration will underestimate the displacement response, although it may capture the maximum acceleration which usually occurs in the forced-vibration phase [Dhakal and Pan 2003]. Higher order vibration modes and local oscillations that have shorter periods are also likely to be excited owing to the high frequency content (more than 100 Hz) of such ground shocks.

3 NUMERICAL STUDY: RC FRAME SUBJECTED TO GROUND SHOCKS

3.1 Target structure and nonlinear models

In order to explore in more detail the structural response to ground shocks, nonlinear time-history analyses of a one-bay two-storey RC frame were conducted. Figure 2 shows the geometrical layout of the frame and its reinforcement details. The frame supports one side of a $5\text{ m} \times 5\text{ m} \times 150\text{ mm}$ slab resting on the beam in each floor. Density of 25 kN/m^3 was used to compute the self-weight of the RC frame and floor, and a live load of 7.5 kN/m^2 was assumed to act on the floors. Shear capacity of the section taken as the sum of the shear contributions from concrete and web reinforcement turned out to be 171.9 kN . Similarly, moment capacity computed according to section analysis was 107.75 kN-m . Assuming the beams to be rigid in axial direction and modelling the frame as a two-degrees of freedom system, frequencies for the first two global horizontal vibration modes were 1.8 Hz and 4.88 Hz , respectively. Similarly, global natural frequency in the vertical direction was approximately 27 Hz . According to preliminary computations based on a generalized SDOF system assuming both ends pinned, the local transverse vibrations of the beams and columns had fundamental frequencies around 4.3 Hz and 43.3 Hz , respectively.

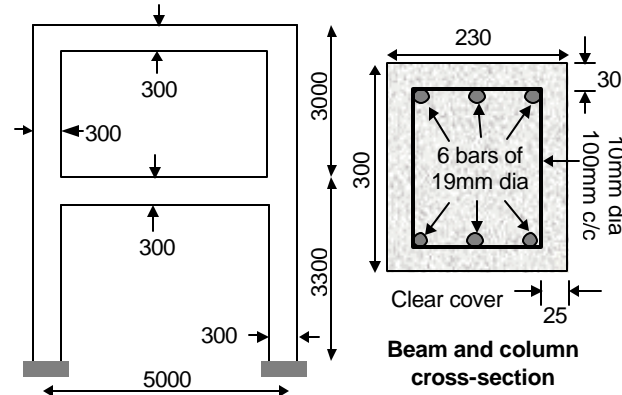


Figure 2 Target 2-storey RC frame

A three-dimensional nonlinear finite-element analysis program *Concrete Model in 3D* (COM3) [Maekawa et al. 1996] was used for numerical investigation. In COM3, nonlinear dynamic computation is based on the direct integration method. Columns and beams were discretized using frame elements, which were analysed by fibre technique. The two-storey RC frame was discretized into 60 elements (i.e. 10 elements for beams and columns in each storey) and each element consisted of 220 parallel fibres. A fibre might contain either concrete only or both concrete and reinforcing bars depending on its position in the cross-section. Following concrete properties were assumed: compressive strength = 30 MPa ; tensile strength = 2 MPa ; Poisson ratio = 0.2 ; compressive strain at peak strength = 0.24% ; and elastic modulus = 24.8 GPa . Similarly, the properties of steel reinforcement were adopted as follows: yield strength = 410 MPa ; ultimate strength = 615 MPa ; breaking strain = 5% ; and Young modulus = 200 GPa . Response of each fibre was computed using nonlinear, cyclic and path-dependent average stress-strain relationships of concrete and reinforcing bars [Okamura and Maekawa 1991]. In the analyses, the beam-column joint was modelled as part of a column member. An equivalent amount of mass was added uniformly throughout the length of the beams to account for the combined live and dead load coming from each floor. Total axial load on each column turned out to be 160 kN , which was around 7.7% of its axial capacity. In order to capture the free-vibration response, ground acceleration records amended to extend well beyond the major shock durations were applied at the fixed supports at the bases of both columns.

3.2 Numerical results and discussion

First, the 2-storey frame was subjected to the representative ground shock detailed earlier. To perceive the response of the frame at closer and farther distances, the analysis was repeated with up-scaled and down-scaled versions of the representative ground shock (i.e., the ground acceleration amplitude was multiplied by 2 and 0.5). Figure 3 shows the time-histories of displacement response of the left column at the floor and roof levels (indicated as 3150 mm and 6150 mm from support) and two mid-storey heights (indicated as 1550 mm and 4650 mm from support). As suspected earlier, the maximum lateral displacement responses occurred during the free-vibration phase. As the displacement histories suggest, the roof vibrated in the fundamental global mode but oscillation of the first floor included the second order global vibration mode, too. Furthermore, the displacement histories of mid-storey points indicated the presence of higher frequency oscillations in addition to the global vibration mode, predominantly in the forced-vibration phase. These high frequency oscillations are attributed to the local vibration modes of the columns which must have been excited because the local modes have higher fundamental frequencies that are closer to the dominant frequency of the ground shock than the fundamental frequencies of the global modes are.

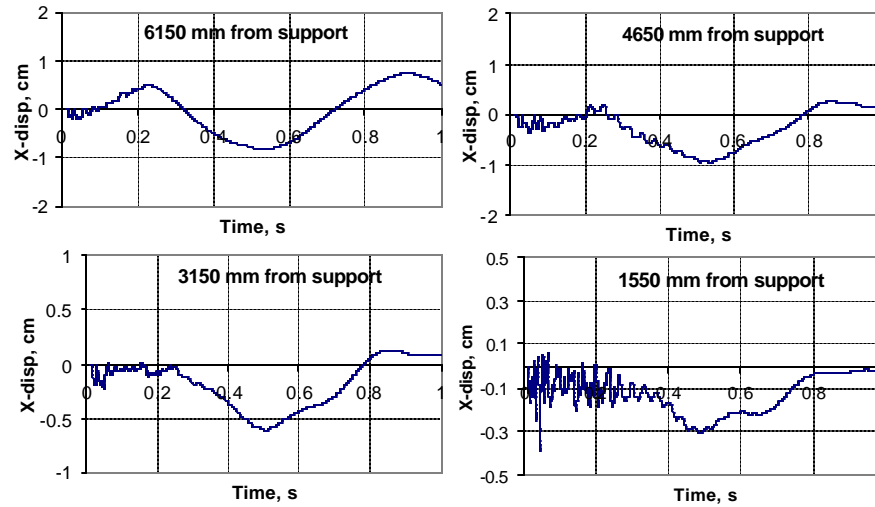


Figure 3 Lateral displacement histories of different points along the left column

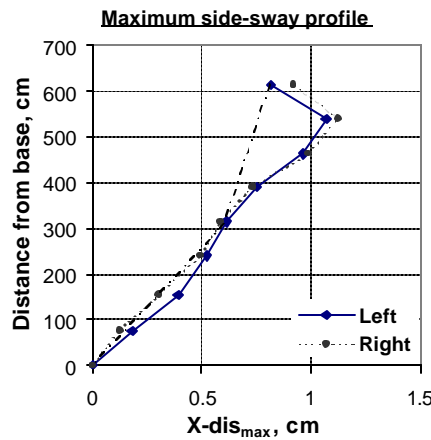


Figure 4 Maximum lateral response profiles along the columns

The existence of local vibration modes can also be illustrated from the absolute maximum lateral displacement profile of the two columns shown in Figure 4. As the lateral displacements at different points in the column reached the maximum value almost simultaneously, the maximum displacement profiles also represent the displaced shapes at the most critical condition. The dashed straight line in

the figure represents the global mode, and column displacement with respect to this line is the contribution of local modes, which is more prominent in the second storey. It can also be observed that most of the global lateral displacement was concentrated in the lower storey, and relative drift of the second storey was much smaller. Note that Figures 3 and 4 are the response of the frame subjected to the representative ground shock, and the results of the analyses using the scaled ground shocks also showed similar trends. Needless to mention, the magnitude of the response expectedly varied depending on the scaling factor.

4 POSSIBLE DAMAGE MECHANISMS

4.1 Shear failure

The high frequency vibration modes are characterised by small displacement and large acceleration. In the forced vibration phase, large acceleration may hence generate significant inertia force which will contribute to the shear force. Therefore, shear failure is likely to happen during the major shock, especially when the ground shock has large impulse because of either a large scale explosion or a short frame-to-explosion distance or both. To verify this logic, the shear responses of the frame at the two supports were monitored in the analyses. Figure 5 illustrates the comparison of induced shear force at the base of both columns with the section shear capacity, i.e. 172 kN. Note that this shear capacity was calculated based on static assumption and may not be applicable in the forced vibration phase because the loading rate is significantly high. The contribution of concrete may increase as faster loading renders the concrete strength higher, whereas the stirrups may not contribute much as the shear cracks are expected to be flatter rather than inclined at 45° as assumed in the computation.

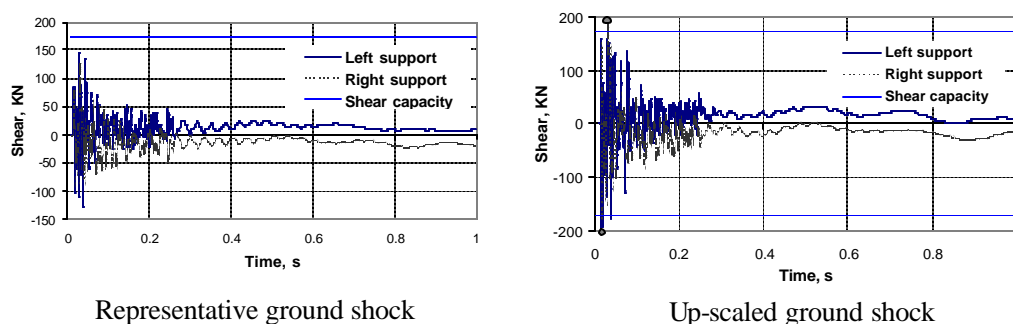


Figure 5 Time-history of column shear forces induced at the base

As indicated, the two plots in the figure correspond to the representative and the up-scaled ground shocks. For both cases, the maximum shear force occurred within the major shock duration, which is because the acceleration and the consequent inertial force are large and contribute significantly to the shear force in the forced-vibration phase. Figure 5 shows that the induced base shear for representative ground shock was less than the shear capacity but the margin was not large enough to completely rule out the possibility of shear failure given that there were uncertainties involved in predicting the shear capacity and location and magnitude of maximum induced shear force. On the other hand, the maximum base shear induced at the base when the frame was subjected to the up-scaled ground shock was higher than the calculated shear capacity warning that shear failure was highly likely to take place in the forced-vibration phase. Similar curve for the analysis with down-scaled shock was not included as it did not provide any additional information to assist the foregoing discussions. Needless to mention, the maximum shear force induced in the column for the down-scaled shock was much less than the shear capacity, and the possibility of shear failure did not exist at all. As mentioned earlier, the up-scaled ground shocks represent closer distance and/or larger explosion, and the foregoing observation hence suggests that structures closer to explosion may undergo shear failure instantly.

4.2 Flexural damage

A structure may not undergo shear failure during the forced-vibration phase if its shear capacity exceeds the maximum shear force induced. In such cases, the large displacement response that occurs after the major shock duration will induce large strain which might inflict damage on the structure. To keep track on the deterioration of materials, strain-histories at some critical locations were monitored continuously. For a qualitative assessment of the damage incurred, maximum tensile and compressive strains experienced by the outermost fibres of the beam and column cross-sections adjacent to the joints are shown in Figure 6. As indicated, the three illustrations in Figure 6 correspond to the down-scaled, representative and the up-scaled ground shocks respectively. As expected, the maximum strains are in the order of the ground shock scaling factor. In all three cases, strains in the beams are larger than those in the columns; the beam in the lower floor experiencing larger strains than the beam in the roof. Along the columns, the strains are the largest at the roof level.

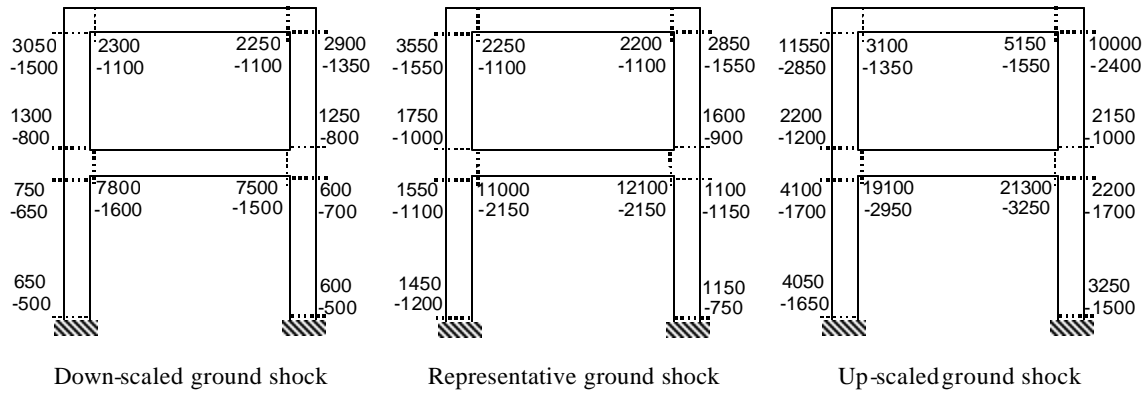


Figure 6 Maximum tensile and compressive strains induced in the frame ($\mu\epsilon$)

For comparison, it is to be remembered that the cracking strain of concrete is approximately $2000 \mu\epsilon$, the yielding strain of the reinforcing bars is approximately $2000 \mu\epsilon$ and the unconfined concrete crushes when the compressive strain enters the range of 2500 - $3500 \mu\epsilon$. In case of the representative ground shock, tensile strains everywhere were larger than the cracking strain but the yielding strain was exceeded only at the beam-ends and the top of the columns, whereas the compressive strains did not exceed the crushing strain. Hence, extensive cracking could be observed and plastic hinges would form at the beam-ends and column-tops. When subjected to the down-scaled ground shock, induced maximum strains were found to be smaller than in the case of representative ground shock, but the strains were still larger than the yielding strain at the beam-ends and columns at the roof level potentially forming plastic hinges there. As strains in all locations exceeded cracking strain, cracks were expected to appear throughout the frame. In case of the up-scaled ground shock, the strains were much larger than in the previous cases, exceeding yielding strain at almost all locations. In addition, the compressive strains at some locations also exceeded the crushing strain suggesting the possible deterioration of sections at these locations in the form of spalling/crushing of concrete. In conclusion, the two-storey frame will be moderately damaged when subjected to the representative and down-scaled ground shocks, but it will be severely damaged when subjected to the up-scaled shock.

It is necessary to recall here that these displacement-induced damages are the features of the free-vibration response, whereas a possibility of shear failure may lie in the forced-vibration phase. Integrating these two mechanisms, it can be said that the frame under the influence of the up-scaled ground shock may first fail in shear in the forced-vibration phase. The results also suggest that the frame, when exposed to the down-scaled ground shock, will not undergo shear failure but it will experience moderate damage in the free-vibration response.

5 CONCEPTUAL DAMAGE ATTENUATION CURVE

Based on the information acquired from the numerical results, overall safety of the frame located at various distances from an explosion can be qualitatively assessed. Figure 7 illustrates the relationship between the quality as well as the nature of damage experienced by the frame and the distance between the frame and the explosion source. The two horizontal dashed lines represent the shear capacity of the frame and its ability to resist critical damage. Hence, these lines are structural features and would shift up/down depending on the toughness of the frame. Similarly, the curved line represents the damaging potential of the explosion and it would also shift up/down depending on the scale of explosion. It is the cross-comparison of these two features that gives information on potential damage the frame might undergo. As the curve shows, the extent of damage expectedly increases as the distance between the explosion and the frame gets smaller. For closer distances, two possible damage mechanisms are identified. Within the shear failure zone D_{sh} , the frame may undergo a sudden shear failure during the forced-vibration phase. The frontier of shear failure zone D_{sh} is the intersection of the solid curved line and horizontal dashed line representing the shear toughness; i.e. D_{sh} depends primarily on the scale of explosion and the shear capacity of the frame. The frame located outside the shear failure zone D_{sh} can safely overcome the forced-vibration phase. Nevertheless, it may still experience severe damage in the free-vibration phase if it is inside the critical damage zone D_{cr} , which is the horizontal distance intercepted by the two horizontal dashed lines on the solid curved line. Beyond the critical damage zone D_{cr} , safety of the frame is guaranteed.

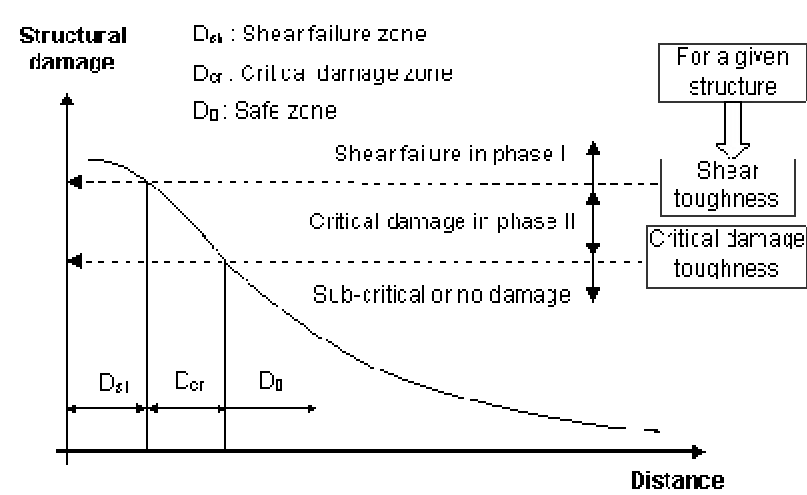


Figure 7 Conceptual damage attenuation curve for the representative frame

Note that there are actually three governing parameters that affect the damage undergone by a structure subjected to explosion induced ground shocks; namely the scale of explosion, the distance between the structure and the explosion, and most importantly, the toughness of the structure. The curve in Figure 7 is drawn assuming the toughness of the frame and the explosion-scale remain unchanged, thus leaving the structure-explosion distance as the only parameter to govern damage. Although such attenuation curves for other structures may be quantitatively different, the conceptual equations derived from the representative frame are applicable to structures in general. Note that for a weaker structure, the two dashed lines will move downwards and the shear failure zone as well as the critical damage zone will be longer, and vice versa. In other words, an explosion may be hazardous for a weak building and, at the same time, harmless for a stronger building. Similarly for a smaller explosion, the curved line will shift downwards and the shear failure zone as well as the critical damage zone will be shorter, and vice versa. In other words, a structure may be safe when exposed to a small explosion, and the same structure may collapse when subjected to a large explosion. Depending on the scale of explosion and the toughness of the structure, the shear failure zone D_{sh} and/or critical damage zone D_{cr} may be long, short or may not exist at all [Dhakal and Pan 2003].

6 CONCLUSION

Explosion-induced ground shocks have some special characteristics such as high frequency, large amplitude and short duration. Due to the impulsive nature of such ground shocks, the maximum drift usually occurs after the major ground shock; i.e. in the free-vibration phase. Hence, analyses aimed to predict structural response to explosion are recommended to cover a time domain much longer than the ground shock duration, and computations only within the shock duration will underestimate the maximum displacement response. The forced-vibration response to a ground shock is dominated by higher frequency vibration modes, which cause a high shear force. On the other hand, free-vibration response is characterized by lower frequency and larger displacement modes thereby creating the possibility of flexural damage. A structure subjected to an explosion may undergo sudden shear failure if it is within the shear failure zone, or may get severely damaged during the free vibration phase if it is within the critical damage zone, or may not be harmed if it is significantly far from the source of explosion.

Future studies should be planned to explore simple but general methods to compute structural toughness and an appropriate ground shock parameter representing the explosion scale. These two parameters can be mutually compared to assess the possibility of shear failure during the major shock. Research is also necessary to establish empirical relationships between the ground shock parameter and structural response parameters at the end of the shock, which would serve as the initial conditions to compute the ensuing free-vibration response. This would relieve the designers from conducting the time-consuming time history dynamic analysis.

ACKNOWLEDGEMENTS:

The work presented in this paper was carried out at the Protective Technology Research Centre of Nanyang Technological University in Singapore. The financial support provided by the Defence Science and Technology Agency, and valuable advices given by Prof. Tso-Chien Pan are gratefully acknowledged.

REFERENCES:

- Dhakal R.P. and Pan T.C. 2003. Response characteristics of structures subjected to blasting induced ground motion. *International Journal of Impact Engineering*. 28(8). 813-828.
- DoD 1992. *Ammunitions and explosives safety standards*. DoD 6055.9-STD, Production and Logistics, Department of Defence, Washington DC, USA.
- Maekawa K., Irawan P. and Okamura H. 1996. Three-dimensional constitutive laws of reinforced concrete. *Proceedings of the International Conference on Applied Concrete Mechanics APCOM*. Seoul, South Korea. 1471-1476.
- Ma G., Hao H. and Zhou Y.X. 1998. Modelling of wave propagation induced by underground explosion. *Computers and Geotechnics*. 22 (3-4). 283-303.
- NATO 1970. *NATO safety principles for the storage of ammunitions and explosives*. Document AC/258-D70. North Atlantic Treaty Organisation, Brussels, Belgium.
- Okamura H. and Maekawa K. 1991. *Nonlinear Analysis and Constitutive Models of Reinforced Concrete*. Gihodo Publication. Tokyo.
- Pan T.C., Dhakal R.P. and Lim C.L. 2003. *Damage assessment of reinforced concrete building frames subjected to explosion induced ground motions*. Final report on PTRC-CSE/LEO/98.02. Protective Technology Research Centre, Nanyang Technological University, Singapore.